Journal of Algorithms and Computation

journal homepage: http://jac.ut.ac.ir

Superpixel-Guided Dark Channel Prior for Efficient Single Image Dehazing

H. Noori*[1], M. H. Gholizadeh[1] and G. Memarzadeh[1]

[1]Department of Electrical Engineering of Vali-e-Asr university of Rafsanjan, Rafsanjan, Iran

ABSTRACT

Outdoor cameras play a vital role in security and social governance systems. However, bad weather can significantly reduce image quality. This can hinder the effectiveness of these systems. This study proposes a new method to remove fog from images captured by outdoor cameras. Unlike traditional methods that analyze small square areas of the image, our approach works with superpixels, which are smarter groupings of pixels. The algorithm first calculates the "dark channel" for each superpixel. The proposed method then merges superpixels with close dark channel values. To prevent unwanted halos around objects after removing the fog, the algorithm applies "guided filtering" to the merged dark channel. The effectiveness is compared to existing methods using various tests that measure image quality. The results show that the proposed method outperforms existing algorithms. This allows for clearer images and improved performance of security governance systems.

ARTICLE INFO

Article history:
Research paper
Received 04, August 2025
Accepted 13, September 2025
Available online 17, September 2025

*Keyword:*Defogging/dehazing, superpixel segmentation, visibility enhancement, dark channel improvement, region aggregating.

AMS subject Classification: 68U10.

*Corresponding author: H. Noori. Email: h.noori@vru.ac.ir

1 Introduction and Literature Review

Images captured in bad weather conditions, i.e. when dust or water particles are suspended in the air, leads to diminished visibility and reduced image contrast. Therefore, these images are unsuitable for advanced computer vision tasks such as remote sensing, target identification, navigation, and video surveillance. Consequently, the mitigation of haze effects through defogging or dehazing techniques represents a significant and expansive area of research [1], with numerous methodologies proposed to address this challenge. Early image defogging methods often relied on supplementary data, such as multiple images captured under different conditions, like different polarization [2], [3] or weather condition [4], [5]. While effective, these approaches come with the drawback of increased complexity and cost associated with acquiring additional information. As a result, the most of researchers have shifted their focus towards single image dehazing, which offers a more cost-effective solution, albeit with limited performance. Single image dehazing algorithms can be broadly categorized into three main groups: fusion-based methods, deep learning-based approaches, and prior-based techniques.

Fusion-based methods [6] - [12] combine multiple enhanced versions of a single hazy image to improve clarity without extra acquisition costs. While promising, they can struggle in dark areas, where combining information is challenging.

Fusion of white balancing and contrast enhancement [6], combinig dark channel prior method with adaptive histogram equalization [7], fusion of gamma corrected multi-scale laplacian images [8], combining several images obtained by multiple patch sizes [9], and fusion of four gamma corrected images with the outcome of color preserving adaptive histogram equalization [10] are proposed. Also, a depth fusion approach for defogging is suggested in [11]. In [12], authors proposed that adaptive exposure multi fusion where three gamma corrected images and an adaptive histogram equalized image are fused using multi-scale Laplacian pyramid.

Deep learning has become a leading approach for single-image dehazing [13] - [24], achieving notable improvements in image restoration. Convolutional Neural Networks (CNNs) are commonly used to learn a mapping from hazy to dehazed images. DehazeNet is presented in [13] to estimate transmission map. In [14], a network including two modules is suggested: the fog inversion module and the image translation module. The network proposed in [15] transforms foggy images into clear ones using a regression framework. Algorithms [16] and [17] have explored the use of generative adversarial networks (GANs) for image dehazing.

In [18], a novel mixed-structure image dehazing network combining Inception and residual modules is introduced. [19] proposes a two-branch network (CNN and vision transformer) to capture global and local features. [20] suggests the DehazeFormer network based on vision transformers. [21] introduces the D4 (Dehazing via Decomposing transmission map into Density and Depth) network, which estimates scattering coefficients and depth maps instead of the transmission map or dehazed image. Due to the scarcity of realistic hazy-clear image pairs, [22] and [23] propose semi-supervised and unsupervised learning methods, respectively. [24] provides a review of deep learning-based image defogging techniques.

Detail enhance attention block is introduced to dehaze in [25].
Although deep learning-based defogging algorithms generally provide reliable results, their high computational demands are attributed to using images as both input and output in the associated networks. Furthermore, these algorithms often require a large dataset for training, which may not always be readily available. Additionally, the presence of light dust or fog, even in clear weather, can introduce uncertainty in establishing ground-truth. Moreover, the efficacy of these algorithms is highly dependent on the dataset used.
Prior-based methods offer a faster and more reliable solution to single-image dehazing [26] - [57]. These methods calculate the dehazed image using a reasonable assumption (prior) and atmospheric scattering model. While they improve visibility significantly, they can fail when the basic assumptions don't hold. A major limitation of these approaches is their reliance on local image patches, typically $r \times r$ neighborhoods. Real-world scenes often have varying haze density and object sizes, which fixed-size patches may not accurately capture, leading to artifacts or limitations in detail recovery.
In [26], author supposed that transmission and surface shading are independent. In [27], author assumed that pixels in small image patches exhibit a one dimensional distribution in RGB color space and finds color lines to dehaze. The algorithm in [27] is extended to non-local patches in [28]. Additionally, the Color Attenuation Prior (CAP) proposed in [29] utilizes a linear model to estimate the depth map for image dehazing. Assuming haze-free images exhibit higher contrast than hazy ones, authors in [30] tried to maximize local image contrast. While visually appealing, the results may not be physically accurate.
In [31], authors assumed that most local patches in outdoor haze-free images contain pixels with very low intensities in at least one color channel, termed dark channel prior (DCP). Utilizing obtained dark channel, the transmission map can be computed. However, the transmission map may suffer a blocking effect, as a result of the local patch-based, defined as an $r \times r$ neighborhood, calculation of the dark channel. Hence, a soft matting algorithm is proposed to tackle this issue. Nevertheless, it is crucial to acknowledge that the soft matting algorithm entails significant computational time. Algorithms in [32] - [47] try to speed up [31] using variety of smoothing algorithms.
Authors in [32] replaced the soft matting algorithm with morphological opening. However, this optimization results in a heightened halo effect. In [33], two de-fogged images are generated in both RGB and YCbCr color spaces and then averaged. The process involves calculating transmission maps for R, G, B and Y channels. To smooth these maps, a gradient derived from a Laplacian filter is subtracted, followed by a mean filter. This method can be computationally more expensive than techniques using a single color space.
Authors in [34], replaced softmatting with morphological opening followed guided filter in [35].
The transmission map in [36] is derived from an improved airlight estimate. This airlight is calculated as a weighted average of airlights obtained from dark and bright channel priors.
Authors in [37], replaced the softmatting with bilateral and adaptive median filters. The method in [38]uses adaptive transmission map smoothing, but it's computationally more expensive than single-map methods. While the Markov Random Field (MRF) approach in [39] offers improved transmission map estimation, it comes at the cost of increased com-

putational complexity. DCP and probability-weighted moments (PWM) are employed to ensure edge preservation during defogging. Compared to [31], [41] achieves improved local consistency by incorporating additional constraints into the dehazing optimization problem. This two-step optimization approach enhances performance but increases computational complexity.

In [42], softmatting is replaced with a novel median filter and edge-preserving smoothing to minimize the halo effect. The method in [43] proposes two defogging algorithms: one for refining the transmission map based on color channel variations, and another for segmenting the image to sky and non-sky regions and defogging each region separately. High dynamic range fog removal is applied to the DCP in [44]. Dark channel is obtained by fusion of two dark channels, calculated separately using median filter and color inversion [45]. The method in [46] uses DCP for low-frequency defogging and combines the result with high frequencies for final image restoration. Also, in [47], a new defogging algorithm is suggested for hyperspectral images.

Stretching the saturation component of foggy images is proposed in [48]. While this method is fast and produces visually pleasing results, it can darken the overall image and may struggle with input images that have bright pixels in all color channels. Similarly, in [49], saturation line prior (SLP) is introduced and dehazing is performed using obtained lines.

A multi-channel convolutional multi-scale Retinex color restoration (MSRCR) based algorithm is proposed in [50]. This method uses guided filtering, Gaussian convolutions, MSRCR enhancement, and white balancing for defogging. However, it's complex and time-consuming. In [51], another method utilizing retinex theory is proposed.

The algorithm in [52] employs a decision image and the dark channel prior to estimate airlight. It then leverages the YCbCr color space, the MSRCR, maximum and minimum filtering to compute the transmission map. Another defogging algorithm is suggested in [53], utilizing adaptive Retinex theory, which yields suitable results but comes at the cost of complexity and time consumption.

This paper proposes a novel approach to single-image dehazing that leverages the dark channel prior within superpixels, overcoming limitations associated with traditional fixed-size ($r \times r$) neighborhoods. Superpixels are clusters of interconnected pixels that exhibit similar characteristics based on specific criteria. In this study, both color and geometrical proximity of pixels are taken into account as criteria for grouping. Once the superpixels are identified, the dark channel of each superpixel is determined, followed by the suggestion to merge superpixels with closely matching dark channel values. Subsequently, the dark channel prior is applied to each merged superpixel to compute the dehazed image. This proposed algorithm calculates the dark channel within the merged superpixel rather than the conventional $r \times r$ neighborhood, thereby preventing blurring and halo effects at image discontinuities. Extensive simulations and comparisons demonstrate the effectiveness of the proposed algorithm.

A superpixel based algorithm is introduced in [57]. The proposed method differs from [57] in several key aspects, as outlined below:

- The proposed method uses the Hue component, which is less affected by fog, to

identify superpixels, while [57] relies on RGB components for this purpose. Since RGB components can become saturated by fog, the superpixels identified by the proposed method are generally more reliable.

- In [57], the superpixels are not merged, leading to a halo effect occurring at the boundaries of the superpixels rather than along the edges. In contrast, the proposed method merges superpixels, which helps alleviate the halo effect.
- The guided filter further diminishes the halo effect, leading to a substantial improvement over the approach outlined in [57].

The remainder of this paper is organized as follows: Modeling an image in foggy weather and the problem statement is discussed in Section 2. Section 3 presents the proposed method. Simulation results and comparison are considered in Section 4. Finally, Section 5 concludes the paper.

2 Preliminaries and Problem Statement

2.1 Fog Imaging Model

Under adverse weather conditions, light reaching a camera is a combination of direct light, attenuated by atmospheric scattering, and indirect light, reflected by suspended particles, creating atmospheric whiteout. This phenomenon is formulated by Koschmieder's law [2]:

$$I(x,y) = J(x,y)t(x,y) + A(1 - t(x,y)), \tag{1}$$

where J represents the haze-free image intensity at pixel location (x, y) and term A captures the atmospheric light. The first term of (1) accounts for attenuation, while the second represents air light. Transmission map t, which is obtained as $t(x,y) = e^{(-\beta d(x,y))}$, depends on scene depth. Where β represents the scattering coefficient of the atmosphere, and d denotes the scene depth.
Building on Eq. (1), defogging can be formulated as an inverse problem where the goal is to recover the haze-free image J from the observed hazy image I. Since the atmospheric light A and transmission map t are unknown, this becomes an ill-posed problem. To tackle the issue of defogging, current methods focus on estimating A and t followed by incorporating them into (1) to obtain J. Many existing methods, such as dark channel prior, assume that specific parameters are similar within local patches.

2.2 Dark Channel Prior

According to the darck channel prior in [31], the dark channel can be expressed as follows:

$$J^{dark}(x,y) = \min_{c\in\{R,G,B\}} \big(\min_{(x_1,y_1)\in\Omega(x,y)} (J^c(x_1,y_1)) \big), \tag{2}$$

where J^{dark} denotes the dark channel of the image J, $\Omega(x, y)$ is a $M \times M$ neighborhood around the pixel at location (x, y), and 'c' in the superscript denotes the color channel of the image. Using the assumption above, equation (1), and asssumption that $t(.,.)$ is constant in each local patch, we have:

$$\min_{c\in\{R,G,B\}} \big(\min_{(x_1,y_1)\in\Omega(x,y)} (\frac{I^c(x_1, y_1)}{A^c}) \big) = \min_{c\in\{R,G,B\}} \big(\min_{(x_1,y_1)\in\Omega(x,y)} (\frac{J^c(x_1, y_1)}{A^c}) \big) + (1 - t(x, y)) \quad (3)$$

Since the dark channel of haze-free images tends to zero, i.e.

$$J^{dark} \to 0 \quad \Longrightarrow \quad \min_{c\in\{R,G,B\}} \big(\min_{(x_1,y_1)\in\Omega(x,y)} (\frac{J^c(x_1, y_1)}{A^c}) \big) \simeq 0 \quad (4)$$

therefore transmission map $t(.,.)$ can be estimated as follows:

$$t(x, y) = 1 - \min_{c\in\{R,G,B\}} \big(\min_{(x_1,y_1)\in\Omega(x,y)} (\frac{I^c(x_1, y_1)}{A^c}) \big) \quad (5)$$

2.3 Problem Statement

As discussed earlier, transmission map, t can be calculated using equation (5), based on the assumption that t remains relatively constant within local patches. In nearly all existing algorithms, a local patch is defined as a rectangular neighborhood of size $r \times r$. However, this assumption may lead to artifacts like the blocking effect, as illustrated in Fig. 1. Fig. 1-a displays a hazy image, while Fig. 1-b illustrates the corresponding dark channel calculated using [31] prior to soft matting. The dehazed image without soft matting is depicted in Fig. 1-c. As evident in the figure, the blocking effect significantly degrades the image quality. The region highlighted by the red rectangle in Fig. 1-b is magnified and shown in Fig. 1-d. Also, the corresponding region in the dehazed image Fig. 1-c is shown in Fig. 1-e. Figure 1-e clearly exhibits significant halo artifacts around depth discontinuities. While numerous algorithms have been proposed to mitigate these artifacts [32] - [47], these algorithms either demand considerable processing time or fail to completely eliminate the halo effect.

As mentioned earlier, most DCP-based algorithms rely on the assumption that the dark channel, calculated as the minimum intensity value within a local traditional $r \times r$ window across all color channels. However, a key question remains: how to determine the optimal value for the window size r? Additionally, Is the rectangular shape of the local neighborhood the most suitable? To improve generalization, this paper proposes the application of DCP to pixels with similar colors within a local neighborhood. Furthermore, to address blocking effects and halo artifacts, the approach involves adjusting the derived dark channel by merging regions with close dark channel values, followed by the utilization of a guided filter. Thus, the contributions of this paper are as follows:

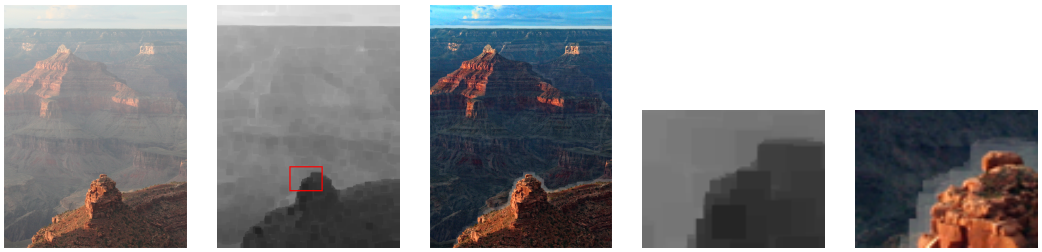

(a) (b) (c) (d) (e)

Figure 1: a) Foggy Image, b) darck channel of foggy image, c) dehazed Image using [31], d) zoomed red rectangle in (b), e) zoomed red rectangle in (c)

- Color-Aware Local Neighborhood: DCP is employed on pixels sharing akin colors within a local neighborhood, thereby augmenting its efficacy across diverse image content and accommodating various neighborhood shapes.
- Refinement of Dark Channel and Guided Filtering: To alleviate blocking artifacts and halo effects, the obtained dark channel is refined through the fusion of regions with analogous values. Subsequently, a guided filter is employed for additional enhancement.
- Extensive experiments demonstrate the effectiveness of the proposed algorithm.

3 Methodology

This section proposes a novel algorithm for single image dehazing. It focuses on identifying the dark channel within local regions of similar color, which we refer to as superpixels. Afterward, it is suggested aggregating regions with highly similar dark channel values. Subsequently, a guided filter is employed to smooth the aggregated dark channel, mitigating any potential halo effects. Finally, estimates for atmospheric light, transmission map, and consequently a defogged image can be calculated.

3.1 Dark Channel Computation

This section introduces a novel algorithm for single image dehazing that leverages superpixel information for robust dark channel estimation. Building on the observation from [28] that haze-free image colors can be approximated by a limited number of distinct colors. Therefore, in this paper, it is proposed to calculate the dark channel within local regions of similar color, referred to as superpixels.Superpixels are clusters of pixels that share similar visual characteristics. They are used in image segmentation to simplify recognition tasks by grouping pixels into meaningful, coherent regions. To identify superpixels, an enhanced version of the simple linear iterative clustering (SLIC) algorithm [58] is proposed. First, we elaborate on the proposed algorithm for superpixel clustering, followed by a discussion on dark channel estimation.

Based on the SLIC algorithm [58], the image is segmented into a user-specified number (k) of approximately equally-sized superpixels. Initially, the algorithm randomly selects k centers in the CIELAB color space, denoted as $C_i = [l_i, a_i, b_i, x_i, y_i]$. Subsequently, for each pixel j in the image, two distances - color distance (d_c) and spatial distance (d_s) - from the center pixel i are computed as follows:

$$d_c = \sqrt{(l_i - l_j)^2 + (a_i - a_j)^2 + (b_i - b_j)^2} \tag{6}$$

$$d_s = \sqrt{(x_i - x_j)^2 + (y_i - y_j)^2} \tag{7}$$

where (x_i, y_j) shows the place of the pixel i. Then these two distances are fused to derive a unified criterion for clustering pixels as follows.

$$D = \sqrt{(\frac{d_c}{N_c})^2 + (\frac{d_s}{N_s})^2} \tag{8}$$

where N_s denotes the maximum spatial distance for clustering pixels, while N_c determines the maximum color distance. To simplify the selection of these two parameters, equation (8) can be expressed as follows:

$$D = \sqrt{(d_c)^2 + (\frac{d_s}{N})^2 m^2} \tag{9}$$

Where N represents the maximum of either the column or row, while m is a parameter that enables us to adjust the balance between color similarity and spatial proximity. When employing the CIELAB color space, the parameter m typically falls within the range of $[1, 40]$ [58].

As noted in [49], fog or haze primarily affects the saturation and brightness components of the HSI color space. To mitigate these effects, it is proposed to utilize only the Hue component for superpixel determination. Consequently, the color distance equation (6) is reformulated as follows:

$$d_c = |h_i - h_j| \tag{10}$$

After determining super pixels, the dark channel can be calculated as follows:

$$J^{dark}(x, y) = \min_{c \in \{R,G,B\}} \big(\min_{(x_1, y_1) \in SP(x,y)} (J^c(x_1, y_1)) \big), \tag{11}$$

where $SP(x, y)$ denotes the superpixel to which pixel (x, y) belongs. Equation (11) indicates that the dark channel prior is applied to superpixels rather than the $r \times r$ rectangular

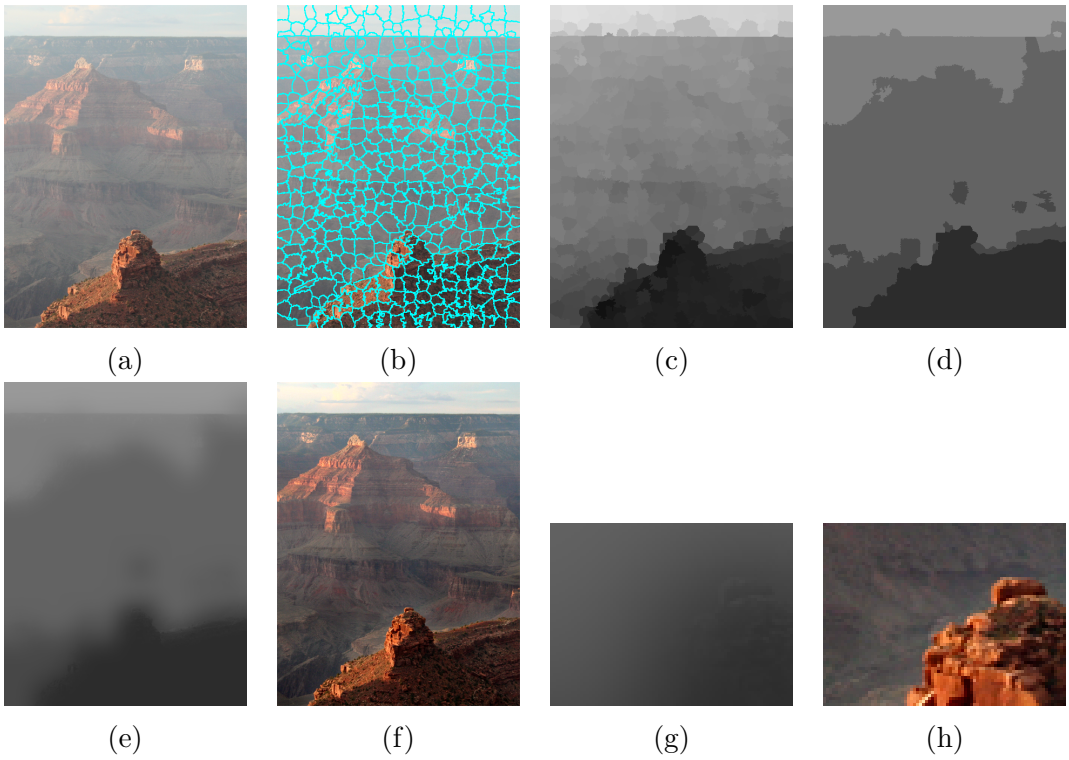

Figure 2: a) Foggy Image, b) Super pixel founded (500), c) dark channel calculated in super pixels, d) aggregated dark channel super pixel, e) guided filter applied to (d), f) dehazed image of the proposed method, g) and h) zoomed red rectangle of fig. 1 of dark channel and the output by the proposed approach

neighborhoods used in previous algorithms. Disappointingly, applying equation (11) to an image doesn't eliminate the blocking effect, as evident in Fig. 2-c. To address the blocking effect, this paper introduces a two-step method. The first step involves aggregating the dark channels of superpixels whose dark channel values, $J^{dark}(x, y)$, fall within 5% of the image's maximum dark channel value. As shown in Fig. 2-d, numerous dark channels of superpixels are consolidated into large one to diminish the halo effect. This amalgamated channel is referred to as the aggregated dark channel. In the second step, to mitigate the halo effect at depth discontinuities, the aggregated dark channel is processed using a guided filter [35]. The guided filter employs a kernel size equal to the square root of the largest superpixel. As illustrated in Fig. 2-e, applying the guided filter to the aggregated dark channel effectively smooths discontinuities. Fig. 2-f presents the final result of the proposed algorithm. As evident in the figure, the dehazed image exhibits no halo effect. Figs. 2-g and 2-h zoom in on the red rectangle in Fig. 1, showcasing the dark channel and the dehazed output from our proposed algorithm, respectively. Notably, Fig. 2-h reveals the absence of halo effect around edge discontinuities.

3.2 Atmospheric Light Estimation

To estimate atmospheric light, the most haze-opaque regions are focused by selecting the top 0.1% brightest pixels from the dark channel. The median value within this set, for each color channel, is chosen as the atmospheric light. Importantly, these pixels might not be the absolute brightest in the entire image [31].

3.3 Calculation of Transmission Medium and Dehazed Image

Once the dark channel is calculated, the transmission medium can be obtained using the following equation:

$$t(x, y) = 1 - \omega J^{dark}(x, y) \tag{12}$$

Where ω is a coefficient (set to 0.95 in this paper) that accounts for the influence of distant areas. Finally, the dehazed image is obtained by applying the following equation, derived from (1):

$$J(x, y)^c = \frac{I(x, y)^c - (1 - t(x, y))A^c}{max\{0.1, t(x, y)\}} \tag{13}$$

The superscript c denotes the color channel. The term in the denominator prevents division by zero. Finally, we can incorporate histogram equalization into the proposed algorithm. While this enhances contrast, it also runs the risk of overcorrection.
The proposed single-step dehazing algorithm is detailed in Algorithm 1. As can be seen from the algorithm, it operates in a non-iterative manner, directly obtaining the entire dehazed image. This characteristic contributes to both its computational efficiency and ease of implementation. Subsequently, we proceed to evaluate and compare the proposed algorithm with conventional methods.

Algorithm 1 Defogging algorithm.

1: Read foggy image I.
2: Find Superpixels of image using equation (7) - (10).
3: Aggregate the superpixels that their dark channel values differs less than 5% of maximum value.
4: Find dark channel of each superpixel and finally the superpixel of the foggy image by (11).
5: Apply guided filter to the calculated dark channel.
6: Calculate atmospheric light.
7: Calculate transmission map employing (12).
8: Obtain the defogged image using (13).

Table 1: Definition of utilized criteria: I and J represent the foggy and defogged images, while μ_I and σ_I denote the average and variance of I. c_1 and c_2 are two constants, and ∇_x represents the differential in the x direction. M and N correspond to the rows and columns of the image.

Ceriterion	Definintion
PSNR	$PSNR = \frac{255}{\sqrt{\frac{1}{M\times N}\sum (J(x,y)-I(x,y))^2}}$
SSIM	$SSIM = \frac{(2\mu_I\mu_J+c_1)(2\sigma_{IJ}+c_2)}{(\mu_I^2\mu_J^2+c_1)(\sigma_I^2\sigma_J^2+c_2)}$
AG	$AG = \frac{1}{(M-1)(N-1)}\sum_{i=1}^{M-1}\sum_{j=1}^{N-1}\sqrt{(\nabla_x J(i,j))^2+(\nabla_y J(i,j))^2}$
FADE	Refer to [59]
NIQE	Refer to [60]

4 Simulation Results

In this section, the proposed algorithm's performance is evaluated and compared to twenty state-of-the-art methods, including five deep learning-based approaches ([13], [20], [15], [23], [25]), two fusion-based methods ([9] and [10]), and thirteen prior-based methods ([26], [29], [30], [31], [42], [48], [49], [32], [33], [36], [45], [57], [51]). The proposed method has only two parameters which are needed to set by user. The first one is the number of superpixels, which is set to 500 for all results in this paper, because the more super pixels like 1000 leads to higher computational time but there is no difference in the final results due to super pixel aggregation. The second one is the kernel size of guided filter, which is set to square root of largest superpixel in the image to avoid halo artifact in the edges (i.e., the second parameter is not set by the user directly in the proposed method, but it can in the guided filter). A six-pronged quantitative comparison is conducted using three reference-based criteria (SSIM [33], PSNR [48], AG [50]), two no-reference criteria (FADE [59], NIQE [60]), and implementation time (details in Table 1). To further assess quality, a qualitative comparison is performed using the original code of each compared algorithm on designated images. However, for a fair implementation time comparison, all methods are re-implemented using MATLAB 2021b on a Lenovo Legion 7 laptop (i7-10750H CPU, 32GB RAM, RTX 2070 Max-Q GPU).

5 Conclusion and Future Works

Finally, this study's proposed method of obtaining dark channel within superpixels, merging areas with close dark channel values, and applying a guided filter to address halo effects has demonstrated superior performance compared to traditional methods and state-of-the-art algorithms. The quantitative evaluation of the proposed algorithm against existing techniques has shown its effectiveness in enhancing image dehazing. Future research efforts could focus on incorporating additional enhancements, such as the application of

saturation line prior to superpixels, to further improve the algorithm's performance and expand its applicability in real-world scenarios. Overall, the study contributes valuable insights to the field of image dehazing and highlights the potential for continued advancements in this area.

References

[1] Z. Chen, Y. Wang, Y. Yang, and D. Liu, "PSD: Principled synthetic-to-real dehazing guided by physical priors," *IEEE/CVF Conference on Computer Vision and Pattern Recognition (CVPR)*, pp. 7176–7185, Jun. 2021, DOI: 10.1109/CVPR46437.2021.00710.

[2] Y. Y. Schechner, S. G. Narasimhan, and S. K. Nayar, "Instant dehazing of images using polarization," *IEEE Computer Society Conference on Computer Vision and Pattern Recognition (CVPR)*, vol. 1, pp. 325–332, Dec. 2001, DOI: 10.1109/CVPR.2001.990493.

[3] Y. Y. Schechner, S. G. Narasimhan, and S. K. Nayar, "Polarization-based vision through haze," *Applied Optics*, vol. 42, no. 3, pp. 511–525, Jan. 2003, DOI: 10.1364/ao.42.000511.

[4] S. G. Narasimhan and S. K. Nayar, "Chromatic framework for vision in bad weather," *IEEE Computer Society Conference on Computer Vision and Pattern Recognition (CVPR)*, pp. 598–605, Jun. 2000, DOI: 10.1109/CVPR.2000.855874.

[5] S. K. Nayar and S. G. Narasimhan, "Vision in bad weather," *7th IEEE International Conference on Computer Vision*, pp. 820–827, Sep. 1999, DOI: 10.1109/ICCV.1999.790306.

[6] C. O. Ancuti and C. Ancuti, "Single image dehazing by multi-scale fusion," IEEE Trans. Image Process., vol. 22, no. 8, pp. 3271–3282, Aug. 2013, DOI: 10.1109/TIP.2013.2262284.

[7] J. M. Guo, J.-Y. Syue, V. R. Radzicki, and H. Lee, "An efficient fusion-based defogging," IEEE Trans. Image Process., vol. 26, no. 9, pp. 4217–4228, Sep. 2017, DOI: 10.1109/TIP.2017.2706526.

[8] A. Galdran, "Image dehazing by artificial multiple-exposure image fusion," Signal Process., vol. 149, pp. 135–147, 2018, DOI: 10.1016/j.sigpro.2018.03.008.

[9] C. Ancuti, C. O. Ancuti, C. De Vleeschouwer, and A. C. Bovik, "Day and night-time dehazing by local airlight estimation," IEEE Trans. Image Process., vol. 29, pp. 6264–6275, 2020, DOI: 10.1109/TIP.2020.2988203.

[10] X. Liu, H. Li and C. Zhu, "Joint contrast enhancement and exposure fusion for real-world image dehazing," *IEEE Transactions on Multimedia*, vol. 24, pp. 3934-3946, 2022, DOI: 10.1109/TMM.2021.3110483.

[11] Y. Wang and C. Fan, "Single Image Defogging by Multiscale Depth Fusion," *IEEE Transactions on Image Processing*, vol. 23, no. 11, pp. 4826–4837, 2014, DOI: 10.1109/TIP.2014.2358076.

[12] W. Mao, D. Zheng, M. Chen, and J. Chen,"Single image defogging via multi-exposure image fusion and detail enhancement," *Journal of Safety Science and Resilience*, vol. 5, I. 1, pp. 37-46, 2024,DOI: 10.1016/j.jnlssr.2023.11.003.

[13] B. Cai, X. Xu, K. Jia, C. Qing, and D. Tao, "DehazeNet: An end-to-end system for single image haze removal," *IEEE Transaction on Image Processing*, vol. 25, no. 11, pp. 5187–5198, 2016, DOI: 10.1109/TIP.2016.2598681.

[14] Q. Guo and M. Zhou, "Progressive domain translation defogging network for real-world fog images," *IEEE Transactions on Broadcasting*, vol. 68, no. 4, pp. 876–885, 2022, DOI: 10.1109/TBC.2022.3187816.

[15] J. Ren, J. Cheng and X. Wang, "An image defogging method based on depth CNN network," *8th International Conference on Control, Automation and Robotics (ICCAR)*, pp. 414–419, Xiamen, China, 2022, DOI: 10.1109/ICCAR55106.2022.9782596.

[16] Y. Cheng, and X. Cheng, "Image defogging algorithm based on deblurgan network," *Frontiers in Computing and Intelligent Systems*, vol. 1, no. 1, pp. 4–8, 2022, DOI:10.54097/fcis.v1i1.1074.

[17] R. R. Choudhary, K K Jisnu, and G. Meena, "Image dehazing using deep learning techniques," *Procedia Computer Science*, vol. 167, pp. 1110-1119, 2020, DOI: 10.1016/j.procs.2020.03.413.

[18] L. P. Lu, Q. Xiong, D. F. Chu and B. R. Xu, "MixDehazeNet : mix structure block For image dehazing network," *International Joint Conference on Neural Networks (IJCNN)*, 2024, DOI: 10.1109/IJCNN60899.2024.10651326.

[19] S. Li, Q . Yuan, Y. Zhang, B. Lv, F. Wei, "Image dehazing algorithm based on deep learning coupled local and global features," *Applied Sciences* vol. 12, I. 17, pp. 1-14, 2022, DOI:10.3390/app12178552.

[20] Y. Song, Z. He, H. Qian and X. Du, "Vision transformers for single image dehazing," *IEEE Transactions on Image Processing*, vol. 32, pp. 1927-1941, 2023, DOI: 10.1109/TIP.2023.3256763.

[21] Y. Yang, C. Wang, R. Liu, L. Zhang, X. Guo, and D. Tao, "Self-augmented unpaired image dehazing via density and depth decomposition," *IEEE/CVF Conference on*

Computer Vision and Pattern Recognition (CVPR), pp. 2037–2046, Jun. 2022, DOI: 10.1109/CVPR52688.2022.00208.

[22] Y. Dong, Y. Li, Q. Dong, H. Zhang, and S. Chen, "Semisupervised domain alignment learning for single image dehazing," *IEEE Transactions on Cybernetics*, vol. 53, no. 11, pp. 7238-7250, Nov. 2023, DOI: 10.1109/TCYB.2022.3221544.

[23] J. Li, Y. Li, L. Zhuo, L. Kuang, and T. Yu, "USID-Net: Unsupervised single image dehazing network via disentangled representations," *IEEE Transaction on Multimedia*, vol. 25, pp. 3587-3601, 2023, DOI: 10.1109/TMM.2022.3163554.

[24] N. Sharma, V. Kumar, and S. K. Singla, "Single image defogging using deep learning techniques: past, present and future," *Archives of Computational Methods in Engineering*, vol. 28, I. 7, pp. 4449 - 4469, 2021, DOI:10.1007/s11831-021-09541-6.

[25] Z. Chen, Z. He, and Z. Lu "DEA-Net: single image dehazing based on detail-enhanced convolution and content-guided attention," *IEEE Transaction on Image Processing*, vol. 33, pp. 1002-1015, 2024, DOI: 10.1109/TIP.2024.3354108.

[26] R. Fattal, "Single image dehazing," *ACM Transactions on Graphics (TOG)*, vol. 27, no. 3, pp. 1–9, New York, 2008, DOI: 10.1145/1360612.1360671.

[27] R. Fattal, "Dehazing using color-lines," *ACM Transactions on Graphics*, vol. 34, no. 1, pp. 1–14, 2014, DOI: 10.1145/2651362.

[28] D. Berman, T. Treibitz and S. Avidan, "Non-local Image Dehazing," *IEEE Conference on Computer Vision and Pattern Recognition (CVPR)*, Las Vegas, NV, USA, pp. 1674-1682, 2016, DOI: 10.1109/CVPR.2016.185.

[29] Q. Zhu, J. Mai and L. Shao, "A Fast Single Image Haze Removal Algorithm Using Color Attenuation Prior," *IEEE Transactions on Image Processing*, vol. 24, no. 11, pp. 3522-3533, Nov. 2015, DOI: 10.1109/TIP.2015.2446191.

[30] R. T. Tan, "Visibility in bad weather from a single image," *IEEE Conference on Computer Vision and Pattern Recognition*, pp. 1–8, 2008, DOI: 10.1109/CVPR.2008.4587643.

[31] K. He, J. Sun and X. Tang, "Single image haze removal using dark channel prior," *IEEE Transactions on Pattern Analysis and Machine Intelligence*, vol. 33, no. 12, pp. 2341–2353, 2011, DOI: 10.1109/CVPR.2009.5206515.

[32] X. He, J. Mao1, Z. Liu, J. Zhou, and Y. Hua, "A fast algorithm for image defogging," *Chinese Conference on Pattern Recognition*, Springer, Berlin, Heidelberg, pp. 149 – 158, 2014, DOI: 10.1007/978-3-662-45643-9_16.

[33] Z. Tufail, Kh. Khurshid, A. Salman, I. F. Nizami, Kh. Khurshid, and B. Jeon, "Improved dark channel prior for image defogging using RGB and YCbCr color space," *IEEE Access*, vol. 6, pp. 32576 – 32587, 2018, DOI: 10.1109/ACCESS.2018.2843261.

[34] A. Kumari, S. Sahdev and S. K. Sahoo, "Improved single image and video dehazing using morphological operation," *International Conference on VLSI Systems, Architecture, Technology and Applications (VLSI-SATA)*, pp. 1–5, 2015, DOI: 10.1109/VLSI-SATA.2015.7050486.

[35] K. He, J. Sun, and X. Tang, "Giuded image filtering," *IEEE Transaction on on Pattern Analysis and Machine Intelligence*, vol. 35, no. 6, pp.1397–1409, 2013, DOI: 10.1109/TPAMI.2012.213.

[36] S. Wen, Y. Zhao, J. Ma, H. k. Lam and H. Wang, "Image Defogging algorithm Based on Image Bright and Dark Channels," *WRC Symposium on Advanced Robotics and Automation (WRC SARA)*, pp. 269–274, 2018, DOI: 10.1109/WRC-SARA.2018.8584245.

[37] Zh. Chen, J. Shen, and P. M. Roth, "Single image defogging algorithm based on dark channel priority," *Journal of Multimedia*, vol. 8, no. 4, pp. 432–438, 2013, DOI: 10.1109/ICCE-Taiwan55306.2022.9869239.

[38] Z. Tufail, Kh. Khurshid, A. Salman, and Kh. Khurshid, "Optimisation of transmission map for improved image defogging," *IET Image Processing*, vol. 13, no. 7, pp. 1161—1169, 2019, DOI: 10.1049/iet-ipr.2018.6485.

[39] F. Guo, H. Peng, and J. Tang, "A new restoration algorithm for single image defogging," *Communications in Computer and Information Science CCPR*, vol. 484, pp. 169–178, 2014, DOI: 10.1007/978-3-662-45643-9_18.

[40] R. M. Yousaf, H. A. Habib, Z. Mehmood, A. Banjar, R. Alharbey, and O. Aboulola, "Single Image Dehazing and Edge Preservation Based on the Dark Channel Probability-Weighted Moments," *Mathematical Problems in Engineering*, vol. 2019, pp. 1–12, 2019, DOI: 10.1155/2019/9721503.

[41] L. He, J. Zhao, N. Zheng and D. Bi, "Haze Removal Using the Difference- Structure-Preservation Prior," *IEEE Transactions on Image Processing*, vol. 26, no. 3, pp. 1063–1075, 2017, DOI: 10.1109/TIP.2016.2644267.

[42] J. Tarel and N. Hautière, "Fast visibility restoration from a single color or gray level image," *2009 IEEE 12th International Conference on Computer Vision*, pp. 2201–2208, 2009, DOI: 10.1109/ICCV.2009.5459251.

[43] A. Sabir, Kh. Khurshid, and A. Salman, "Segmentation-based image defogging using modified dark channel prior," *EURASIP Journal on Image and Video Processing*, vol. 6, pp. 1– 14, 2020, DOI: 10.1186/s13640-020-0493-9.

[44] M. I. Anwar and A. Khosla, "Vision enhancement through single image fog removal," *Engineering Science and Technology, an International Journal*, vol. 20, no. 3, pp. 1075–1083, 2017, DOI: 10.1016/j.jestch.2016.11.015.

[45] F. Yang and Y. Hu, "Improved dark channel prior for image defogging," *2022 International Conference on Artificial Intelligence and Computer Information Technology (AICIT)*, pp. 1–4, Yichang, China, 2022, DOI: 10.1109/AICIT55386.2022.9930190.

[46] C. Qin and X. Gu, "A single image dehazing method based on decomposition strategy," *Journal of Systems Engineering and Electronics*, vol. 33, no. 2, pp. 279-293, April 2022, DOI: 10.23919/JSEE.2022.000029.

[47] X. Kang, Z. Fei, P. Duan and S. Li, "Fog model-based hyperspectral image defogging," *IEEE Transactions on Geoscience and Remote Sensing*, vol. 60, pp. 1-12, 2022, DOI: 10.1109/TGRS.2021.3101491.

[48] S. E. Kim, T. H. Park and I. K. Eom, "Fast Single Image Dehazing Using Saturation Based Transmission Map Estimation," *IEEE Transactions on Image Processing*, vol. 29, pp. 1985–1998, 2021, DOI: 10.1109/TIP.2019.2948279.

[49] P. Ling, H. Chen, X. Tan, Y. Jin and E. Chen,"Single image dehazing using saturation line prior," *IEEE Transactions on Image Processing*, vol. 32, pp. 3238-3253, 2023, DOI: 10.1109/TIP.2023.3279980.

[50] W. Zhang, L. Dong, X. Pan, J. Zhou, L. Qin and W. Xu, "Single image defogging based on multi-channel convolutional MSRCR," *IEEE Access*, vol. 7, pp. 72492-72504, 2019, DOI: 10.1109/ACCESS.2019.2920403.

[51] H. Noori, M. H. Gholizadeh, H. Khodabakhshi Rafsanjani, "Digital image defogging using joint Retinex theory and independent component analysis," *Computer Vision and Image Understanding*, vol. 245, pp. 1-16, 2024, DOI: 10.1016/j.cviu.2024.104033.

[52] J. Wang, K. Lu, J. Xue, N. He and L. Shao, "Single Image Dehazing Based on the Physical Model and MSRCR Algorithm," *IEEE Transactions on Circuits and Systems for Video Technology*, vol. 28, no. 9, pp. 2190–2199, 2018, DOI: 10.1109/TCSVT.2017.2728822.

[53] G. Qingqing, W. Xiangping, W. Ke, W. Shuang and H. Shaowei, "Adaptive retinex image defogging algorithm based on the depth of field information," *IEEE Intl Conf on Dependable, Autonomic and Secure Computing, Intl Conf on Pervasive Intelligence and Computing, Intl Conf on Cloud and Big Data Computing, Intl Conf on Cyber Science and Technology Congress*, pp. 1–7, Falerna, Italy, 2022, DOI: 10.1109/DASC/PiCom/CBDCom/Cy55231.2022.9927853.

[54] F. Guo, J. Yang, Z. Liu, and J. Tang, "Haze removal for single image: A comprehensive review," *Neurocomputing*, vol. 537, pp. 85-109, 2023, DOI: 10.1016/j.neucom.2023.03.061.

[55] Y. Xu, J. Wen, L. Fei and Z. Zhang, "Review of video and image defogging algorithms and related studies on image restoration and enhancement," *IEEE Access*, vol. 4, pp. 165-188, 2016, DOI: 10.1109/ACCESS.2015.2511558.

[56] J. Wang, H. Wang, Y. Sun and J. Yang,"Improved Retinex-theory-based low-light image enhancement algorithm," *Applied science*, vol. 13, I. 14, pp. 1-14, 2023, DOI: 10.3390/app13148148.

[57] M. Yang, Z. Li and J. Liu, "Super-pixel based single image haze removal," *2016 Chinese Control and Decision Conference (CCDC)*, Yinchuan, China, 2016, pp. 1965-1969, DOI: 10.1109/CCDC.2016.7531305.

[58] R. Achanta, A. Shaji, K. Smith, A. Lucchi, P. Fua and S. Süsstrunk, "SLIC superpixels compared to state-of-the-art superpixel methods," *IEEE Transactions on Pattern Analysis and Machine Intelligence*, vol. 34, no. 11, pp. 2274-2282, Nov. 2012, DOI: 10.1109/TPAMI.2012.120.

[59] L. K. Choi, J. You and A. C. Bovik, "Referenceless Prediction of Perceptual Fog Density and Perceptual Image Defogging," *IEEE Transactions on Image Processing*, vol. 24, no. 11, pp. 3888-3901, Nov. 2015, DOI: 10.1109/TIP.2015.2456502.

[60] A. Mittal, R. Soundararajan and A. C. Bovik, "Making a 'Completely Blind' Image Quality Analyzer," *IEEE Signal Processing Letters*, vol. 20, no. 3, pp. 209-212, March 2013, DOI: 10.1109/LSP.2012.2227726.